



Journal of Applied and Computational Mechanics



Research Paper

A New Quantum-computing-based Algorithm for Robotic Arms and Rigid Bodies' Orientation

Nadjet Zioui¹, Yousra Mahmoudi^{1,2,3}, Aicha Mahmoudi⁴, Mohamed Tadjine⁵, Said Bentouba⁶

¹ Department of Mechanical Engineering, Université du Québec à Trois-Rivières & Institut de Recherche sur l'Hydrogène, 3351 Boulevard des Forges, Trois-Rivières, QC G8Z 4M3, Canada, Email: nadjet.zioui@uqtr.ca

² Laboratoire RECITS, Université de la Science et de la Technologie Houari Boumediene, BP 32 Bab Ezzouar, 16111, Algiers, Algeria, Email: yousra.mahmoudi@uqtr.ca

³ Département Hydraulique Urbaine, École Nationale Supérieure d'Hydraulique Arbaoui Abdallah, 29 Route de Soumaâ, Blida, Algeria

⁴ Projet Véo, Université de Sherbrooke, 2500 Boulevard de l'Université, Sherbrooke, QC J1K 2R1, Canada, Email: aicha.mahmoudi@usherbrooke.ca

⁵ Laboratoire de Commande des Processus, Ecole Nationale Polytechnique, Algiers, Algeria, Email: mohamed.tadjine@g.enp.edu.dz

⁶ Faculty of Engineering and Science, Western Norway University of Applied Sciences Bergen, 5063, Norway, Email: said.bentouba@hvl.no

Received June 01 2021; Revised July 03 2021; Accepted for publication July 09 2021.

Corresponding author: N. Zioui (nadjet.zioui@uqtr.ca)

© 2021 Published by Shahid Chamran University of Ahvaz

Abstract. Quantum computing model of robotic arm orientation is presented. Spherical and vector coordinates, a homogenous rotation matrix, Pauli gates and quantum rotation operators are used to formulate the orientation model and establish a new algorithm. The quantum algorithm uses a single qubit to compute orientation and has the advantage of operation reversibility. This was validated for a SCARA robot and a five-joints articulated robotic arm. The obtained results show the effectiveness of the proposed methodology.

Keywords: Quantum computing; Robotic arm orientation model; Yaw, pitch and roll angles; Spherical coordinates; Quantum rotation operators.

1. Introduction

Quantum computing and algorithms development is no longer a purely academic research area. As a result of recent methodological advances, adaptations of classical computing concepts to quantum calculations are now foreseeable in several engineering fields. However, most of the studies published so far focus primarily on solving systems of linear differential equations [1], [2], finding roots [3], [4], or solving non-linear differential equations [5], [7], [8]. Actual experiments are presented in rare cases [6]. Very little attention has been given to reducing the number of qubits and therefore resources used. Much research in quantum computing is focused on optimization problems that arise in classical physics. The Grover algorithm for database search [9] continues to find application to searches for optima [10].

Modelling is one of the most important steps in systems control. Simulations using models provide insight into system behaviour, but the model is often also the main basis for successful implementation of computerized control strategies.

For making sense of the dynamic behaviour of systems and signal processing, two important tools are the Laplace transform and the Fourier. Quantum versions of the Laplace transform [11], [12], as well as the Fourier transform [13] have been described. Fourier transform tools are already available in several quantum simulation tools [14].

Despite the progress, much room remains for improvements and innovations that reduce the computing resources needed and to optimize existing tools [15], [16] or bring new concepts and tools into the field. In this regard, we are interested in the potential of quantum spin for application to systems modelling.

Robotic arm modelling methods have been covered extensively in the literature. A robotic arm model presents the end effector position, orientation, speed, and acceleration relative to the base frame for given joint values and successive derivatives, and vice versa. For kinematic modelling, the most popular way of setting the successive joint frames and establishing the homogenous matrix that links the joint variables to the Cartesian variables x , y and z has been the Denavit-Hartenberg method [17], [18], [19], [20], [21], [22]. Because of their compact expression, quaternions and dual quaternions are popular methods of modelling rigid robotic arm position and orientation [23], [24], [25], [26], [27], [28].

We have not found any study that describes the application of quantum computing to robotic arm modelling. This appears to be a research and development opportunity with a future. In this article, we present a quantum model for determining robotic arm orientation based on spherical representation and basic quantum rotations. This provides a very compact algorithm for robotic arm rotation using only one qubit. The proposed model is validated on a SCARA and a five-joints articulated robotic arms.



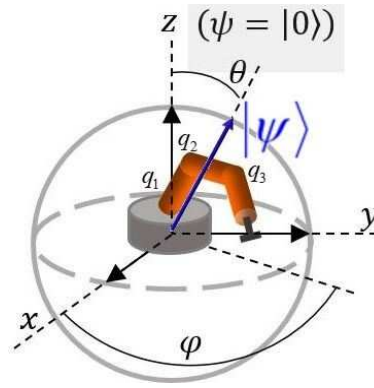


Fig. 1. Spherical representation of a qubit Q (known as the Bloch sphere) along with the orientation of a robotic arm.

2. Tools and materials

In this study, robotic arm orientation is modelled in terms of pitch, roll and yaw angles using spherical coordinates and a homogenous rotation matrix. The basic principles of quantum computing, including Pauli matrices, linear algebra, as well as rotation matrix operators are defined below to establish the association with orientation modelling formalism as illustrated in Fig. 1.

2.1 Quantum computing basics

Quantum computing principles are derived mainly from quantum mechanics and principles introduced by Dirac [29], [30], [31].

2.1.1 The qubit

The fundamental unit of information in quantum computing is the qubit. Unlike the binary bit, of which the admissible values are 0 or 1 only, a qubit, also called a ket, is intelligible in the superposition state of 0 and 1. It can be simultaneously 0 and 1 and any complex combination of 0 and 1. Symbolized as $|\psi\rangle$, it evolves in a two-dimensional Hilbert space.

$$|\psi\rangle = \alpha|0\rangle + \beta|1\rangle \tag{1}$$

where α and β are complex numbers such that $|\alpha|^2 + |\beta|^2 = 1$, $|0\rangle$ and $|1\rangle$ are the orthogonal eigenstates of $|\psi\rangle$, corresponding to logic states 0 and 1, respectively. $|\alpha|^2$ represents the probability of the qubit being found in the eigenstate $|0\rangle$ and $|\beta|^2$ represents the probability of finding it in eigenstate $|1\rangle$. The superposition principle represented above (1) is at the heart of the parallel processing property of quantum computing. For an input x , a qubit processing a function $f(x)$ can work out simultaneously many different results. The qubit state can be represented also by the following vector (see Fig. 1).

$$|\psi\rangle = \begin{pmatrix} \psi_1 \\ \psi_2 \end{pmatrix} = \begin{pmatrix} \alpha \\ \beta \end{pmatrix} \tag{2}$$

The eigenstates $|0\rangle$ and $|1\rangle$ are represented by $(1 \ 0)^T$ and $(0 \ 1)^T$.

2.1.2 The joint state of a system of qubits

The joint state of two qubits $|\psi\rangle = \alpha|0\rangle + \beta|1\rangle$ and $|\psi'\rangle = \alpha'|0\rangle + \beta'|1\rangle$ can be represented by the tensor product of the two qubit states. This product is denoted by $|\psi\psi'\rangle$, and can be computed as follows:

$$|\psi\psi'\rangle = |\psi\rangle \otimes |\psi'\rangle = \alpha\alpha'|00\rangle + \alpha\beta'|01\rangle + \beta\alpha'|10\rangle + \beta\beta'|11\rangle \tag{3}$$

For three qubits $|\psi_1\rangle = \alpha_1|0\rangle + \beta_1|1\rangle$, $|\psi_2\rangle = \alpha_2|0\rangle + \beta_2|1\rangle$ and $|\psi_3\rangle = \alpha_3|0\rangle + \beta_3|1\rangle$, the joint state is denoted $|\psi_1\psi_2\psi_3\rangle$ and can be computed as follows:

$$|\psi_1\psi_2\psi_3\rangle = |\psi_1\rangle \otimes |\psi_2\rangle \otimes |\psi_3\rangle = \alpha_1\alpha_2\alpha_3|000\rangle + \alpha_1\alpha_2\beta_3|001\rangle + \alpha_1\beta_2\alpha_3|010\rangle + \alpha_1\beta_2\beta_3|011\rangle + \beta_1\alpha_2\alpha_3|100\rangle + \beta_1\alpha_2\beta_3|101\rangle + \beta_1\beta_2\alpha_3|110\rangle + \beta_1\beta_2\beta_3|111\rangle \tag{4}$$

Entanglement is said to occur when the state of a qubit system cannot be expressed as a tensor product of the qubit states. Entangled qubit have strongly correlated states. Information about one of them give immediately information about the other.

2.1.3 Measuring a qubit

The inner product of two qubit states $|\psi\rangle = \alpha|0\rangle + \beta|1\rangle$ and $|\psi'\rangle = \alpha'|0\rangle + \beta'|1\rangle$ is denoted $\langle\psi, \psi'\rangle$. The result is a complex number, given by:

$$\langle\psi, \psi'\rangle = \alpha^*\alpha' + \beta^*\beta' \tag{5}$$

where x^* is the complex conjugate of x . The inner product of a qubit state and itself $\langle\psi, \psi\rangle$ gives a number $\text{Re}(\alpha)^2 + \text{Re}(\beta)^2$. The inner product of a state $|0\rangle$ or $|1\rangle$ with a qubit state $|\psi\rangle$ will give the corresponding coefficient α or β .

The outer product between two qubit states $|\psi\rangle = \alpha|0\rangle + \beta|1\rangle$ and $|\psi'\rangle = \alpha'|0\rangle + \beta'|1\rangle$ is denoted $|\psi\rangle\langle\psi'|$. It yields a matrix given by the inner products as follows:



$$|\psi\rangle\langle\psi| = \begin{pmatrix} \alpha \\ \beta \end{pmatrix} (\alpha^* \quad \beta^*) = \begin{pmatrix} \alpha\alpha^* & \alpha\beta^* \\ \beta\alpha^* & \beta\beta^* \end{pmatrix} = U \quad (6)$$

Measuring a qubit is synonymous with reading the information stored in the qubit system or determining if the qubit state is 0 or 1. This is expressed as a probability. For instance, the qubit defined in equation (1) will be found in the state $|0\rangle$ with probability $|\alpha|^2$ or in the state $|1\rangle$ with probability $|\beta|^2$. $\langle 0, \psi |^2$ and $\langle 1, \psi |^2$ symbolize this measurement.

It is also possible to compute the probability of obtaining a bit string $|a_1 a_2 \dots a_n\rangle$ from measuring a qubit state $|\psi\rangle$ as $\langle a_1 a_2 \dots a_n | \psi \rangle^2$, and to measure partial state. For instance, the probability of finding the first qubit in state $|0\rangle$ in a three-qubit system would be $\sum_{(a_2, a_3) \in \{0,1\}^2} \langle 0 a_2 a_3 | \psi \rangle^2$. The qubit system thus measured must then be normalized: $\sum_{(a_2, a_3) \in \{0,1\}^2} \langle 0 a_2 a_3 | \psi \rangle |0 a_2 a_3\rangle$.

2.1.4 Common gates and operators

Time evolution of qubit is always given by Unitary Linear Transformations (or operator). In this section, we present the most important 2×2 Hermitian operators that are very useful in quantum computing.

2.1.4.1 The X gate

The X gate, the quantum version of the NOT gate, can be represented by the operator X as shown below. Note that application of this operator to the state vector $(1 \ 0)^T$ or the Z axis gives the state vector $(0 \ 1)^T$ or the X axis and vice versa.

$$X \equiv \begin{pmatrix} 0 & 1 \\ 1 & 0 \end{pmatrix} \quad (7)$$

2.1.4.2 The CNOT gate

The CNOT or controlled NOT gate negates the target qubit if and only if the control qubit state is 1. This gate can be expressed as follows:

$$\text{CNOT} \equiv |00\rangle\langle 00| + |01\rangle\langle 01| + |10\rangle\langle 11| + |11\rangle\langle 10| \quad (8)$$

2.1.4.3 The CCNOT gate

The CCNOT or controlled CNOT gate can be seen as a reversible version of the AND gate. It negates the target qubit if and only if both control qubits are of status 1.

2.1.4.4 The Y gate

The Y gate is defined using either of the equations below. Application of the operator expressed in equation (10) to state $(1 \ 0)^T$ or the Z axis results in state $(0 \ i)^T$ or the Y axis.

$$Y \equiv -i|0\rangle\langle 1| + i|1\rangle\langle 0| \quad (9)$$

$$Y \equiv \begin{pmatrix} 0 & -i \\ i & 0 \end{pmatrix} \quad (10)$$

2.1.4.5 The Z gate

The Z operator can be expressed using the equations given below. Note that application of this operator to state $(1 \ 0)^T$ or the Z axis will leave this state unchanged.

$$Z \equiv |0\rangle\langle 0| - |1\rangle\langle 1| \quad (11)$$

$$Z \equiv \begin{pmatrix} 1 & 0 \\ 0 & -1 \end{pmatrix} \quad (12)$$

2.1.4.6 The H gate

The H or Hadamard gate defined below can be perceived as rotation around the axis between x and z.

$$\begin{cases} H|0\rangle = |+\rangle \\ H|1\rangle = |-\rangle \end{cases} \quad (13)$$

$$H \equiv \frac{1}{\sqrt{2}} \begin{pmatrix} 1 & 1 \\ 1 & -1 \end{pmatrix} \quad (14)$$

2.1.4.7 The rotation gates

Three rotation gates can be used in quantum computing: $R_x(\theta)$, $R_y(\theta)$ and $R_z(\theta)$, which represent the three basic rotations of angle θ around the axes x, y and z, respectively. Rotations can be performed using the following operators:



$$R_x(\theta) = \begin{pmatrix} C\frac{\theta}{2} & -iS\frac{\theta}{2} \\ -iS\frac{\theta}{2} & C\frac{\theta}{2} \end{pmatrix} \tag{15}$$

$$R_y(\theta) = \begin{pmatrix} C\frac{\theta}{2} & -S\frac{\theta}{2} \\ S\frac{\theta}{2} & C\frac{\theta}{2} \end{pmatrix} \tag{16}$$

$$R_z(\theta) = \begin{pmatrix} e^{-i\frac{\theta}{2}} & 0 \\ 0 & e^{i\frac{\theta}{2}} \end{pmatrix} \tag{17}$$

where C stands for the cosine function and S stands for the sine function.

2.1.5 Quantum algorithm representation

2.1.5.1 The rotation gates

Quantum algorithms are often represented as circuits with qubits represented by horizontal lines and gates or operators represented by boxes. The initial state of the qubit, usually $|0\rangle$, is indicated on the left end of the line. A circuit is understood by reading from left to right. The operation $NOT|0\rangle$ is represented below:

2.1.5.2 The Pauli matrices

The Pauli matrices are basic Hermitian matrices that allow definition of any quantum operator by means of linear transformation. They are defined as follows:

$$\sigma_0 = I = \begin{pmatrix} 1 & 0 \\ 0 & 1 \end{pmatrix}; \sigma_1 = \sigma_x = \begin{pmatrix} 0 & 1 \\ 1 & 0 \end{pmatrix}; \sigma_2 = \sigma_y = \begin{pmatrix} 0 & -i \\ i & 0 \end{pmatrix}; \sigma_3 = \sigma_z = \begin{pmatrix} 1 & 0 \\ 0 & -1 \end{pmatrix} \tag{18}$$

Rotation operators (15), (16) and (17) can be written, for instance, using the Pauli gates as the following: $R_x(\theta) = C\theta - iS\theta\sigma_x$, $R_y(\theta) = C\theta - iS\theta\sigma_y$ and $R_z(\theta) = C\theta - iS\theta\sigma_z$.

It should be noted that the Pauli matrices σ_x , σ_y and σ_z are the matrix representations of the X, Y and Z gates. These matrices verify the properties shown below. Note also that the first property $\sigma_j^2 = \sigma_0$ supports the gate reversibility principle.

$$\begin{cases} \sigma_j^2 = \sigma_0, j = 1, 2, 3 \\ \sigma_x\sigma_y = -\sigma_y\sigma_x = i\sigma_z \\ \sigma_y\sigma_z = -\sigma_z\sigma_y = i\sigma_x \\ \sigma_z\sigma_x = -\sigma_x\sigma_z = i\sigma_y \end{cases} \tag{19}$$

2.2 Models of robotic arm orientation

Robotic arms orientation can be expressed using several approaches. In this article, we use spherical coordinates, yaw, roll and pitch angles and the Denavit-Hartenberg rotation matrix.

2.2.1 Spherical coordinates

In its representation as spherical coordinates, the orientation of a vector is expressed using two angles φ and θ as illustrated in Fig. 3.

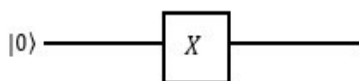


Fig. 2. Basic example of a quantum circuit.

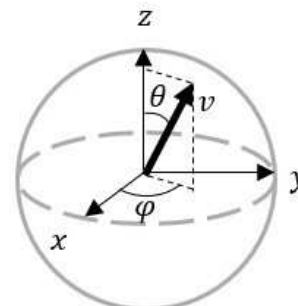


Fig. 3. The spherical representation of a vector.



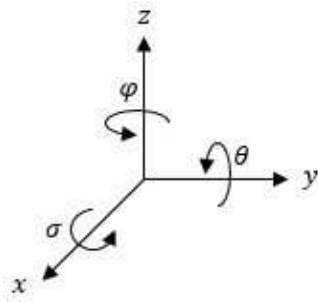


Fig. 4. Yaw, pitch and roll angles.

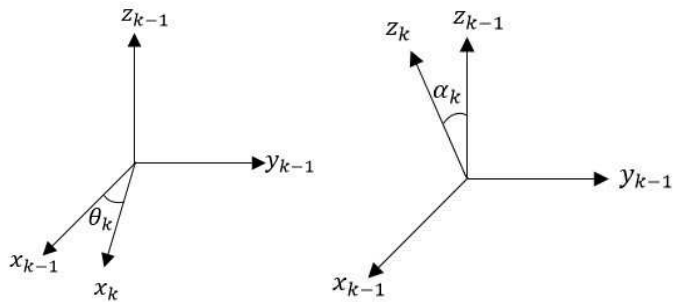


Fig. 5. The Denavit-Hartenberg angles θ_k and α_k .

The rotation matrix for the spherical representation is given below.

$$R = \begin{pmatrix} \cos \theta \cos \varphi & -\sin \varphi & \sin \theta \cos \varphi \\ \cos \theta \sin \varphi & \cos \varphi & \sin \theta \sin \varphi \\ -\sin \theta & \cos \theta & \cos \theta \end{pmatrix} \tag{20}$$

2.2.2 Yaw, pitch and roll angles

In 3D space, any arbitrary orientation of a mechanical body can be decomposed and represented using the elementary rotations around the x, y and z axes as shown in Fig. 4. [17]

Rotation φ (around the z axis) is called the roll angle, rotation θ (around the y axis) is called the pitch angle, and rotation σ (around the x axis) is called the yaw angle.

The rotation matrix of yaw, pitch and roll is represented below. It is the product $R_z R_y R_x$ of the three elementary rotation matrices (22, 23 and 24) [17].

$$R = \begin{pmatrix} C\theta C\varphi & -C\sigma S\varphi + S\sigma S\theta C\varphi & S\sigma S\varphi + C\sigma S\theta C\varphi \\ C\theta S\varphi & C\sigma C\varphi + S\sigma S\theta S\varphi & -S\sigma C\varphi + C\sigma S\theta S\varphi \\ -S\theta & S\sigma C\theta & C\sigma C\theta \end{pmatrix} \tag{21}$$

where $S\sigma$, $S\theta$ and $S\varphi$ are, respectively, $\sin \sigma$, $\sin \theta$ and $\sin \varphi$, and $C\sigma$, $C\theta$ and $C\varphi$ are, respectively, $\cos \sigma$, $\cos \theta$ and $\cos \varphi$.

$$R_x(\sigma) = \begin{pmatrix} 1 & 0 & 0 \\ 0 & C\sigma & -S\sigma \\ 0 & S\sigma & C\sigma \end{pmatrix} \tag{22}$$

$$R_y(\theta) = \begin{pmatrix} C\theta & 0 & S\theta \\ 0 & 1 & 0 \\ -S\theta & 0 & C\theta \end{pmatrix} \tag{23}$$

$$R_z(\varphi) = \begin{pmatrix} C\varphi & -S\varphi & 0 \\ S\varphi & C\varphi & 0 \\ 0 & 0 & 1 \end{pmatrix} \tag{24}$$

It should be noted that when the yaw angle is zero, the representation in Fig. 4 becomes equivalent to the spherical coordinates illustrated in Fig. 3, and that matrix (21) will be equivalent to matrix (20) for $\sigma = 0$.

2.2.3 Homogenous matrix

Denavit-Hartenberg formulation provides a 4x4 matrix containing a 3x3 rotation matrix R that allows passage from a frame L_{k-1} to a frame L_k as expressed below using the angles θ_k and α_k defined in Fig. 5.

$$R = \begin{pmatrix} \cos \theta_k & -\cos \alpha_k \sin \theta_k & \sin \alpha_k \sin \theta_k \\ \sin \theta_k & \cos \alpha_k \cos \theta_k & -\sin \alpha_k \cos \theta_k \\ 0 & \sin \alpha_k & \cos \alpha_k \end{pmatrix} \tag{25}$$



3. Methodology

3.1 Determining robot arm orientation from the homogenous matrix

It should be noted at the outset that with the coordinates of any pair of unit vectors (columns of matrix R), matrix (25) should provide enough information to express arm orientation, since the third unit vector of the base can be determined using the right-hand rule. For instance, with $u_x = (\cos \theta_k \sin \theta_k \ 0)^T$ and $u_z = (\sin \alpha_k \sin \theta_k \ -\sin \alpha_k \cos \theta_k \ \cos \alpha_k)^T$, which are the first and last columns of matrix R , the third unit vector of the base is determined using the vector product $u_y = -u_x \times u_z$, giving complete information on arm orientation.

Moreover, there is redundancy embedded in vectors u_x and u_z . The term $\cos \theta_k$ (the first coordinate of unit vector u_x) appears also in the second coordinate of unit vector u_z , just as $\sin \theta_k$ (the second coordinate of u_x) also appears in the first coordinate of u_z . On the other hand, $\cos \alpha_k$ and $\sin \alpha_k$ give complete information on unit vector u_z , $\cos \theta_k$ and $\sin \theta_k$ on unit vector u_x , based on spherical representation.

A single base vector could be expressed, for example the z axis in spherical coordinates, as in matrix (20). But this expression would need to be completed, since rotation around an arbitrary vector will not be perceived in this representation. Yaw, pitch and roll would provide a more complete representation of orientation since the yaw angle represents essential information.

3.2 Spherical coordinates in the quantum representation

The most intuitive way to model the orientation of a robotic arm in quantum computing is to use basic rotation matrices or the spins. Such a procedure involves identifying the spherical angles of the arm then applying successive rotations to the initial qubit state, which is $|0\rangle \equiv (1 \ 0)^T$ (the z or joint axis). The quantic model will emerge from rotating φ around the z axis, followed by rotation θ around the y axis, giving the result shown below.

$$|\psi_R\rangle = R_y(\theta)R_z(\varphi)|0\rangle \cong C\theta|0\rangle + S\theta e^{i\varphi}|1\rangle \equiv \begin{pmatrix} C\theta \\ S\theta e^{i\varphi} \end{pmatrix} \tag{26}$$

$$u_z = \begin{pmatrix} \sin \theta \cos \varphi \\ \sin \theta \sin \varphi \\ \cos \theta \end{pmatrix} = \begin{pmatrix} \sin \theta \begin{pmatrix} \cos \varphi \\ \sin \varphi \end{pmatrix} \\ \cos \theta \end{pmatrix} \tag{27}$$

$$e^{i\varphi} = \begin{pmatrix} \cos \varphi \\ \sin \varphi \end{pmatrix} \tag{28}$$

The sign \cong in (26) means supposed to be, or considered as being.

Relation (26) defines mainly the spin around an arbitrary vector, this model is fundamental and could have been used directly to implement the quantic model of robotic arm orientation, since the equivalence to 3D space can be established naturally using the third column of matrix R (20), and modifying it according to relations shown in (27) and (28). However, the reader can notice that a zero or $k\pi$ value of the pitch angle θ in this model will result in loss of information for the roll angle φ . Therefore, it appears more appropriate to apply successive unit spin operators to the initial quantum state $|0\rangle$ (respectively the $|1\rangle$ quantum state) in order to obtain the orientation of the z -axis (respectively the x -axis) orientation. Model (29) results from this described procedure. This last model will be used for the simulation of the illustrative cases of study.

$$|\psi\rangle = R_z(\varphi)R_y(\theta)|0\rangle \equiv \begin{pmatrix} e^{-i\varphi} & 0 \\ 0 & e^{i\varphi} \end{pmatrix} \begin{pmatrix} \cos \theta & -\sin \theta \\ \sin \theta & \cos \theta \end{pmatrix} \begin{pmatrix} 1 \\ 0 \end{pmatrix} = C\theta|0\rangle e^{-i\varphi} + S\theta e^{i\varphi}|1\rangle \tag{29}$$

Since by spherical convention θ is measured from the z axis to xy plane, the Denavit-Hartenberg joint angle is that measured from the x axis to said z axis. Moreover, the several frames thus defined might differ from the frame used in quantum computing. This detail must not be overlooked when formulating the robotic quantum model. An illustrative example will be presented for this purpose.

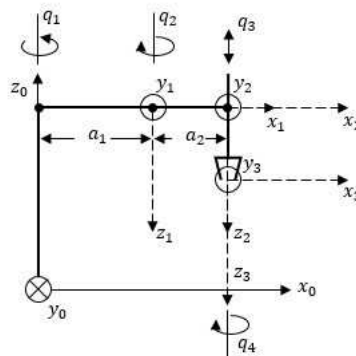


Fig. 6. SCARA robot arm joints and frames [32], [33].



4. Simulation, validation and discussion

In the sections that follow, we present the results obtained for the implementation and validation of robotic arm orientation models for two types of robots.

4.1 Case study 1

A SCARA robotic arm was considered. The several Denavit-Hartenberg frames $L_k (k = 1,2,3)$ were established as illustrated in Fig. 6.

It is apparent in Fig. 6 that expressing the orientation of the end effector relative to the base frame involves the following transformations and corresponding rotations:

- A rotation q_1 around the z axis
- A rotation π around the x axis
- A rotation $-q_2$ around the z axis
- A rotation $-q_4$ around the z axis

These transformations collectively allow the orientation of the robotic arm to be performed using the two basic rotation operators $R_z(q_1 - q_2 - q_4)$ and $R_x(\pi)$.

On the other hand, the orientation of the SCARA robotic arm is obtained using the 3x3 Denavit-Hartenberg matrix (30) [17], which is expressed in spherical form in matrix (31).

$$R_0^3 = \begin{pmatrix} C_{1-2-4} & S_{1-2-4} & 0 \\ S_{1-2-4} & -C_{1-2-4} & 0 \\ 0 & 0 & 1 \end{pmatrix} \tag{30}$$

$$R_0^3 = \begin{pmatrix} C_1 & -S_1 & 0 \\ S_1 & C_1 & 0 \\ 0 & 0 & 1 \end{pmatrix} \begin{pmatrix} 1 & 0 & 0 \\ 0 & -1 & 0 \\ 0 & 0 & -1 \end{pmatrix} \begin{pmatrix} C_2 & -S_2 & 0 \\ S_2 & C_2 & 0 \\ 0 & 0 & 1 \end{pmatrix} \begin{pmatrix} C_4 & -S_4 & 0 \\ S_4 & C_4 & 0 \\ 0 & 0 & 1 \end{pmatrix} = \begin{pmatrix} C_{1-2-4} & S_{1-2-4} & 0 \\ S_{1-2-4} & -C_{1-2-4} & 0 \\ 0 & 0 & 1 \end{pmatrix} \tag{31}$$

where C_1, S_1, C_{1-2-4} and S_{1-2-4} respectively refer to $\cos(q_1), \sin(q_1), \cos(q_1 - q_2 - q_4)$ and $\sin(q_1 - q_2 - q_4)$.

The spherical coordinates can be identified as $\theta = \pi$ and $\varphi = q_1 - q_2 - q_4$. From model (29), the qubit state of the orientation therefore can be defined as follows:

$$|\psi\rangle \equiv e^{-i(q_1 - q_2 - q_4)} \cos \pi |0\rangle + e^{i(q_1 - q_2 - q_4)} \sin \pi |1\rangle = -e^{-i(q_1 - q_2 - q_4)} |0\rangle \tag{32}$$

This expression conserves the coordinates along the three axes. The term $e^{-i(q_1 - q_2 - q_4)}$ embodies the base frame x axis coordinates, the negative sign indicating that they are oriented in the negative direction of the z axis represented by the state $|0\rangle$.

4.2 Case study 2

Here, we consider a five-axis articulated robotic arm, using the Denavit-Hartenberg frame represented in Fig. 7. [17]

Without considering initial joint positions, the orientation of the end effector in the base frame can be expressed by obtaining the following transformations:

- Rotation q_1 around the z axis
- Rotation q_2 around the y axis
- Rotation q_3 around the y axis
- Rotation q_4 around the y axis

The robotic arm orientation therefore can be determined using the two basic rotation operators $R_z(q_1)$ followed by $R_y(q_2 + q_3 + q_4 + \pi)$. The additional angle π , in the spin around the y axis expression, results from angles q_2, q_3 and q_4 being measured from the horizontal base plane, while the angle θ from the spherical coordinates is measured from the vertical axis. The applicable angle is therefore $\pi/2$. However, there is an extra $\pi/2$ due to the z axis in the Denavit-Hartenberg formulation being orthogonal to the z axis in the quantum representation. Fig. 8 illustrates the relationship between the Denavit-Hartenberg angles and the spherical representation for this specific case.

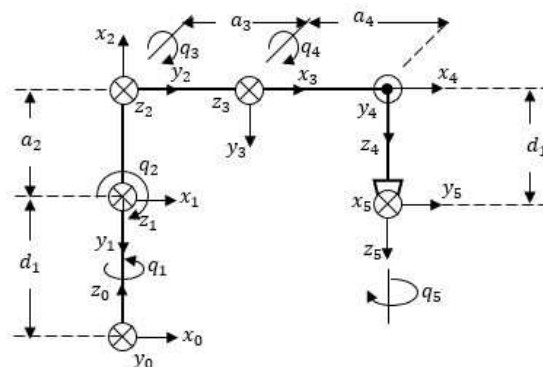


Fig. 7. Five-jointed robotic arm articulations and frames.



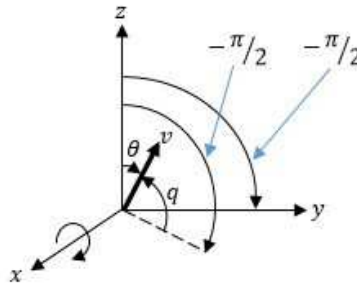


Fig. 8. Relationship between Denavit-Hartenberg θ_k and the spherical coordinates angle θ .

The corresponding 3x3 orientation matrices for this specific five-axis robotic arm [17] are shown below.

$$R_0^5 = \begin{pmatrix} C_1 C_{234} C_5 + S_1 S_5 & -C_1 C_{234} S_5 + S_1 C_5 & -C_1 S_{234} \\ S_1 C_{234} C_5 - C_1 S_5 & -S_1 C_{234} S_5 - C_1 C_5 & -S_1 S_{234} \\ -S_{234} C_5 & S_{234} S_5 & -C_{234} \end{pmatrix} \tag{33}$$

$$R_0^5 = \begin{pmatrix} C_1 & -S_1 & 0 \\ S_1 & C_1 & 0 \\ 0 & 0 & 1 \end{pmatrix} \begin{pmatrix} C_2 & 0 & S_2 \\ 0 & 1 & 0 \\ -S_2 & 0 & C_2 \end{pmatrix} \begin{pmatrix} C_3 & 0 & S_3 \\ 0 & 1 & 0 \\ -S_3 & 0 & C_3 \end{pmatrix} \begin{pmatrix} C_4 & 0 & S_4 \\ 0 & 1 & 0 \\ -S_4 & 0 & C_4 \end{pmatrix} \begin{pmatrix} 1 & 0 & 0 \\ 0 & -1 & 0 \\ 0 & 0 & -1 \end{pmatrix} = \begin{pmatrix} C_1 C_{234} C_5 + S_1 S_5 & -C_1 C_{234} S_5 + S_1 C_5 & -C_1 S_{234} \\ S_1 C_{234} C_5 - C_1 S_5 & -S_1 C_{234} S_5 - C_1 C_5 & -S_1 S_{234} \\ -S_{234} C_5 & S_{234} S_5 & -C_{234} \end{pmatrix} \tag{34}$$

in which C_5 , S_5 , C_{234} and S_{234} , respectively, refer to $\cos(q_5)$, $\sin(q_5)$, $\cos(q_2 + q_3 + q_4)$ and $\sin(q_2 + q_3 + q_4)$.

Using model (29), the qubit state of the orientation can be defined as shown below, considering the spherical coordinates $\theta = q_2 + q_3 + q_4 + \pi$ and $\varphi = q_1$.

$$|\psi\rangle \equiv e^{-iq_1} \cos(q_2 + q_3 + q_4 + \pi)|0\rangle + e^{iq_1} \sin(q_2 + q_3 + q_4 + \pi)|1\rangle = -e^{-iq_1} \cos(q_2 + q_3 + q_4)|0\rangle - e^{iq_1} \sin(q_2 + q_3 + q_4)|1\rangle \tag{35}$$

Notice that the term e^{-iq_1} specifies the base-frame x-axis coordinates, while the negative sign, resulting from the angle $+\pi$, indicates that the orientation of the z-axis, represented by the state $|0\rangle$, points towards the negative direction.

The result can be obtained by determining the unit rotations using the relation shown below.

$$|\psi\rangle \equiv R_z(q_1)R_z(q_2 + q_3 + q_4 + \pi)|0\rangle \tag{36}$$

4.3 Simulation results and discussion

In the following discussion, one qubit is used to describe the orientation of each robotic arm. The quantum programs were implemented considering $|0\rangle$ as the initial state of the qubit. The quantum circuit for case study 1 is illustrated in Fig. 9.

The simulation was run using $q_1 = \pi/6$, $q_2 = \pi/36$ and $q_4 = \pi/12$. This yielded the qubit state $|\psi\rangle = (-0.985 - 0.174i)|0\rangle + (0.0 + 0.0i)|1\rangle$. The result was validated by comparing it to the theoretical result obtained using orientation matrix (30). For the same angles, the orientation is given below.

$$R_0^3 = \begin{pmatrix} C_{\frac{\pi}{6} \frac{\pi}{36} \frac{\pi}{12}} & S_{\frac{\pi}{6} \frac{\pi}{36} \frac{\pi}{12}} & 0 \\ S_{\frac{\pi}{6} \frac{\pi}{36} \frac{\pi}{12}} & -C_{\frac{\pi}{6} \frac{\pi}{36} \frac{\pi}{12}} & 0 \\ 0 & 0 & -1 \end{pmatrix} = \begin{pmatrix} 0.985 & 0.174 & 0 \\ 0.174 & -0.985 & 0 \\ 0 & 0 & -1 \end{pmatrix} \tag{37}$$

The qubit state vector is oriented along the z axis. The negative sign indicates orientation in the opposite direction. Finally, since the x axis coordinates are conserved, the y axis can be determined using the right-hand rule.

The quantum circuit for case study 2 is illustrated in Fig. 10.

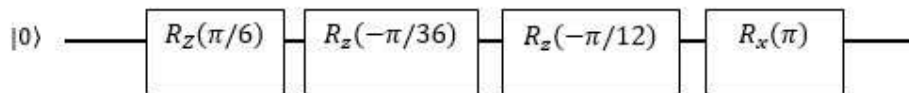


Fig. 9. Quantum circuit for the SCARA robot arm orientation model.

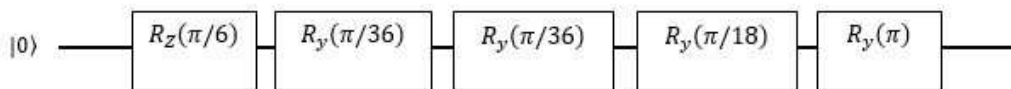


Fig. 10. Quantum circuit for implementing the five-jointed robotic arm orientation model.



The simulation was run using $q_1 = \pi/6$, $q_2 = \pi/36$, $q_3 = \pi/36$ and $q_4 = \pi/18$. This yielded the qubit state $|\psi\rangle = (-0.814 + 0.47i)|0\rangle + (-0.296 - 0.171i)|1\rangle$. The result is validated by comparing to the theoretical result obtained using orientation matrix (34). For the same angles, the z axis orientation (third column) is given below:

$$Z_0^5 = \begin{pmatrix} -C_1 S_{234} \\ -S_1 S_{234} \\ -C_{234} \end{pmatrix} = \begin{pmatrix} -0,296 \\ -0,171 \\ -0,94 \end{pmatrix} \tag{38}$$

The qubit state vector result indicates that x axis orientation information is conserved since component $|1\rangle$ corresponds to the x and y coordinates of the z axis in relation (38). The negative sign again indicates the vector orientation along the z axis. Finally, the component $|0\rangle$ of the qubit state norm result $\sqrt{(0.814)^2 + (0.47)^2}$ corresponds to the z component in relation (38), thus validating the result.

The former results relate to the validation of the model for specific orientations. In order to generalize the results, a five order polynomial generated motion is considered [18].

For the simulation, the quantum model (29) is written as (39).

$$|\psi\rangle = (\text{Re}(\alpha) + \text{Im}(\alpha))|0\rangle + (\text{Re}(\beta) + \text{Im}(\beta))|1\rangle \tag{39}$$

where $\text{Re}(\alpha) = C\theta C\varphi$, $\text{Im}(\alpha) = -C\theta S\varphi$, $\text{Re}(\beta) = S\theta C\varphi$ and $\text{Im}(\beta) = S\theta S\varphi$ are determined by identification.

In order to extract the coordinates of the z-axis from model (39), the following is used:

$$Z_0^n = \begin{pmatrix} \text{Re}(\beta) \\ \text{Im}(\beta) \\ -\frac{\text{Re}(\alpha)}{C\varphi} \text{ or } \frac{\text{Im}(\alpha)}{S\varphi} \end{pmatrix} \tag{40}$$

Figures 11.b and 12 illustrate the orientation of the z-axis using the D-H formalism and the quantum model method for the first and second cases of studies, respectively. The following initial values were considered for the fifth polynomial approach:

For the first case of study:

Initial values: $q_{1i} = \frac{\pi}{6} \text{ rad}$, $q_{2i} = \frac{\pi}{36} \text{ rad}$ and $q_{4i} = \frac{\pi}{12} \text{ rad}$.

Final values: $q_{1f} = \frac{\pi}{3} \text{ rad}$, $q_{2f} = \frac{\pi}{2} \text{ rad}$ and $q_{4f} = \frac{\pi}{4} \text{ rad}$.

For the second case of study:

Initial values: $q_{1i} = \frac{\pi}{6} \text{ rad}$, $q_{2i} = \frac{\pi}{36} \text{ rad}$, $q_{3i} = \frac{\pi}{36} \text{ rad}$ and $q_{4i} = \frac{\pi}{18} \text{ rad}$.

Final values: $q_{1f} = \frac{\pi}{4} \text{ rad}$, $q_{2f} = \frac{\pi}{3} \text{ rad}$, $q_{3f} = \frac{\pi}{18} \text{ rad}$ and $q_{4f} = \pi \text{ rad}$.

Figures 11 and 12 support the validity of the model for continuous time operations as the results of the quantum model match those obtained using the classic methods, namely the D-H formalism. From Fig. 11.b, it can be perceived that the z axis points towards the opposite direction of the z axis of base frame. This can be concluded by the coordinates' values z_x and z_y that are very close to 0 and $z_z = -1$. Moreover, the results in Fig. 11.a, show how the orientation of the x axis has been successfully extracted from the resulting qubit state as the results match those obtained using the classic 3x3 orientation matrix. The presented results in Fig. 11 and Fig. 12 reinforce the validity of the quantum model for continuous time and curves.

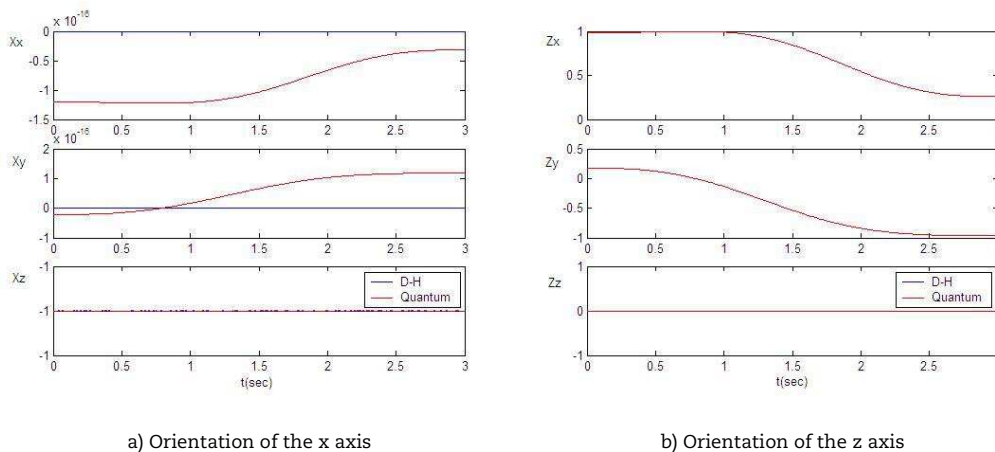


Fig. 11. Simulation results for the orientation of the robot using the D-H and the quantum models, for the SCARA robotic arm: (a) Orientation of the x axis; (b) Orientation of the z axis.



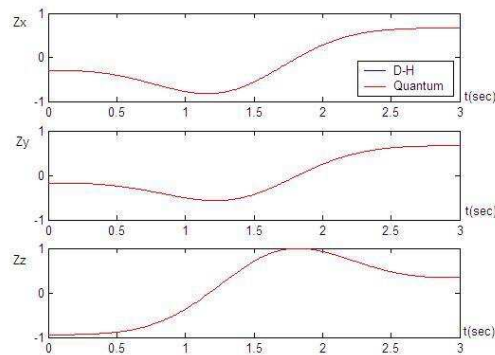


Fig. 12. Simulation results for the orientation of the robot using the D-H and the quantum models, for the five joints articulated robot arm.

5. Conclusion

Quantum computing algorithm of the orientation of robotic arms using a model based on spherical coordinates to define basic rotations can be envisaged. The quantum model was validated for a SCARA and five joints articulated robot arms. A single qubit was sufficient to describe forward orientation comparably to the usual 3x3 orientation matrices. The paper proposed a successful way to extract orientation information from the resulting qubit state. This quantum model is a step forward towards quantum simulation and future software for mechatronics systems. The main strengths for this model are the reduced computing resources as only one qubit allowed the implementation and the validation of the orientation of robotic arms. The other main advantage of this new model is the reversibility of the quantum operators that might potentially be exploited in the inverse models computation. The inverse model and position models are under development for future work and studies.

Author Contributions

Nadjet Zioui contributed to conceptualization, methodology, software, validation, formal analysis, data curation, writing - original draft, visualization, supervision, and project administration. Yousra Mahmoudi contributed to investigation, resources and writing - original draft. Aicha Mahmoudi contributed to conceptualization, methodology, resources, writing - original draft, visualization and project administration. Tadjine Mohamed contributed to conceptualization, methodology, writing - review & editing. Said Bentouba contributed to visualization, writing - review & editing.

Acknowledgments

Nadjet Zioui would like to make special Acknowledgments to all her professors from Les Vergers School, Albassatine Aldjadida School, Technicum of Birkhadem and École Nationale Polytechnique of Algiers.

Conflict of Interest

The authors declared no potential conflicts of interest with respect to the research, authorship, and publication of this article.

Funding

The authors received no financial support for the research, authorship, and publication of this article.

Nomenclature

a_k	The k^{th} link length of a robotic arm in the Denavit-Hartenberg formulation	x, y and z	The coordinates of v in a specified base frame
CCNOT	The controlled CNOT gate	X	The X gate
CNOT	The controlled NOT gate	Y	The Y gate
d_k	The k^{th} link offset of a robotic arm in the Denavit-Hartenberg formulation	Z	The Z gate
H	The Hadamard gate	α_k	The k^{th} link twist angle of a robotic arm in the Denavit-Hartenberg formulation
L_k	The frame associated with the k^{th} joint	θ_k	The k^{th} joint angle of a robotic arm in the Denavit-Hartenberg formulation
$R_x(\theta)$	The rotation gate at angle θ around the x axis	$\sigma_0, \sigma_x, \sigma_y$ and σ_z	The Pauli matrices
$R_y(\theta)$	The rotation gate at angle θ around the y axis	$ \psi\rangle$	Qubit state
$R_z(\theta)$	The rotation gate at angle θ around the z axis	$ 0\rangle$	The first base vector in quantum computing
T_0^k	The matrix transformation from the L_0 base frame to frame L_k	$ 1\rangle$	The second base vector in quantum computing
v	An arbitrary vector		


References


- [1] Berry, D.W., High-Order Quantum Algorithm for Solving Linear Differential Equations, *Journal of Physics A: Mathematical and Theoretical*, 47(10), 2014, 105301.
- [2] Cao, Y., Daskin, S., Frankel, S., Kais, S., Quantum Circuit Design for Solving Linear Systems of Equations, *Molecular Physics*, 110(1), 2012, 1675-1680.





- [3] Cai, X.D., Weedbrook, C., Su, Z.E., Chen, M., Cu, M.J., Zhu, L., Li, N.L., Liu, C.Y., Lu, J.W.P., Experimental Quantum Computing to Solve Systems of Linear Equations, *Physical Review Letters*, 110, 2013, 230501.
- [4] Nagata, K., Nakamura, T., *Quantum Algorithm for the Root-Finding Problem*, Chapman University, Springer, 2018.
- [5] Leyton, S.K., Osborne, T.J., A Quantum Algorithm to Solve Nonlinear Differential Equations, *arXiv: 0812.4423v1*, 2008.
- [6] Xin, T., Wei, S., Cui, J., Xiao, J., Arrazola, I., Lamata, L., Kong, X., Lu, D., Solano, E., Long, G., A Quantum Algorithm for Solving Linear Differential Equations: Theory and Experiment, *Physical Review A*, 101(1), 2018, 032307.
- [7] Terno, D.R., Nonlinear Operations in Quantum-Information Theory, *Physical Review A*, 59(5), 1999, 3320.
- [8] Daoud, E.A., Quantum Computing for Solving a System of Nonlinear Equations over GF(q), *The International Arab Journal of Information Technology*, 4(3), 2007, 201-205.
- [9] Grover, L.K., A Fast Quantum Mechanical Algorithm for Database Search in STOC '96, *Proceedings of the twenty-eighth annual ACM symposium on Theory of Computing*, 1996.
- [10] Singhal, A., Chatterjee, A., *Grover's Algorithm*, 2018.
- [11] Pimentel, D.R.M., Castro, A.S., A Laplace Transform Approach to the Quantum Harmonic Oscillator, *European Journal of Physics*, 34(1), 2013, 199.
- [12] Sarikaya, M.Z., Alp, N., q-Laplace Transform on Quantum Integral, *Kragujevac Journal of Mathematics*, 47, 2023, 153–164.
- [13] Jorrand, P., Transformée de Fourier Quantique - Algorithmes, Notes de cours - Module Informatique Quantique, UJF Grenoble, 2006.
- [14] Quantum Fourier Transform, Qiskit, [Online]. Available: <https://qiskit.org/textbook/ch-algorithms/quantum-fourier-transform.html>. [Accessed 10 05 2021].
- [15] Wossnig, L., Zhao, Z., Prakash, A., A Quantum Linear System Algorithm for Dense Matrices, *Physical Review Letters*, 120, 2017, 050502.
- [16] Kyriienko, O., Quantum Inverse Iteration Algorithm for Programmable Quantum Simulators, *npj Quantum Information*, 6, 2020, 7.
- [17] Schilling, R.J., *Fundamentals of Robotics: analysis and control*, Simon & Schuster Trade, 1996.
- [18] Khalil, E.D.W., *Modélisation, Identification et commande des Robots*, Hermès Science, 1999.
- [19] Siciliano, B., Sciavico, L., Villani, L., Oriolo, G., *Robotics: Modelling, Planning and Control*, Springer Science & Business Media, 2010.
- [20] Sciavico, L., Siciliano, B. *Modelling and Control of Robot Manipulators*, Springer Science & Business Media, 2012.
- [21] Forstner, W.B.P.W., *Photogrammetric computer vision: statistics, geometry, orientation and reconstruction*, Springer, 2016.
- [22] Mittal, I.N.R., *Robotics and control*, Tata McGraw-Hill, 2003.
- [23] Blösch, M., *An Introduction to 3D Orientations and Quaternions*, ETH Zurich, Zurich, 2015.
- [24] Adorno, B.V., Robot Kinematic Modeling and Control Based on Dual Quaternion Algebra - Part I: Fundamentals, Department of Electrical Engineering, Federal University of Minas Gerais, Brazil, 2017.
- [25] Al Attar, A., Kormushev, P., Kinematic-Model-Free Orientation Control for Robot Manipulation Using Locally Weighted Dual Quaternions, *Robotics*, 9(4), 2020, 76.
- [26] Barbic, J., Quaternions and Rotations in CSCI 420, *Computer Graphics*, 2020.
- [27] Chen, L., Zielinska, T., Wang, J., Ge, W., Solution of an Inverse Kinematics Problem Using Dual Quaternions, *International Journal of Applied Mathematics and Computer Science*, 30(2), 2020, 351–361.
- [28] Valverde, A., Tsiotras, P., Spacecraft Robot Kinematics Using Dual Quaternions, *Robotics*, 7(4), 2018, 64.
- [29] Griffiths, R.B., *Consistent Quantum Theory*, Cambridge University Press, 2002.
- [30] McMahon, D., *Quantum Computing Explained*, Wiley - IEEE, 2007.
- [31] Abhijith, J., Adedoyin, A., Ambrosiano, J., Anisimov, P., Bärtschi, A., Casper, W., Chennupati, G., Coffrin, C., Djidjev, H., Gunter, D., Karra, S., Lemons, N., Lin, S., Malyzhenkov, A., *Quantum Algorithm Implementations for Beginners*, ArXiv, 2018.
- [32] Chikh, N.Z.L., *Design, realization and control of a SCARA robot*, National Polytechnic School (ENP), Algiers, Algeria, 2006.
- [33] Zioui, N., Mahmoudi, A., Mahmoudi, Y., Rezgui, A., A Comparative Study of Performances between the Sliding Modes and the Trust Control Strategies for an Articulated Robotic Arm Position Control, *International Journal of Mechatronics and Mechanical Engineering*, 21(1), 2021, 64-72.


ORCID iD

Nadjat Zioui  <https://orcid.org/0000-0003-1579-4053>

Yousra Mahmoudi  <https://orcid.org/0000-0002-0048-4194>

Aicha Mahmoudi  <https://orcid.org/0000-0003-4595-2112>

Mohamed Tadjine  <https://orcid.org/0000-0001-9715-2673>

Said Bentouba  <https://orcid.org/0000-0003-3859-8717>



© 2021 Shahid Chamran University of Ahvaz, Ahvaz, Iran. This article is an open access article distributed under the terms and conditions of the Creative Commons Attribution-NonCommercial 4.0 International (CC BY-NC 4.0 license) (<http://creativecommons.org/licenses/by-nc/4.0/>).

How to cite this article: Zioui N., Mahmoudi Y., Mahmoudi A., Tadjine M., Bentouba S. A New Quantum-computing-based Algorithm for Robotic Arms and Rigid Bodies' Orientation, *J. Appl. Comput. Mech.*, 7(3), 2021, 1836–1846. <https://doi.org/10.22055/JACM.2021.37611.3048>

Publisher's Note Shahid Chamran University of Ahvaz remains neutral with regard to jurisdictional claims in published maps and institutional affiliations.

